Local Softness versus Local Density of States as Reactivity Index

Loc Thanh Nguyen,[†,‡] Frank De Proft,[‡] Montserrat Cases Amat,[‡] Gregory Van Lier,[‡] Patrick W. Fowler,[§] and Paul Geerlings*[,‡]

Group of Computational Chemistry, Faculty of Chemical Engineering, HoChiMinh City University of Technology, HoChiMinh City, Vietnam, Onderzoeksgroep Algemene Chemie, Vrije Universiteit Brussel, Pleinlaan 2, B-1050 Brussels, Belgium, and School of Chemistry, University of Exeter, Stocker Road, Exeter EX4 4QD, U.K.

Received: February 14, 2003

The definition of softness and local softness using the density of states (DOS) and local density of states (LDOS) given by Yang and Parr for metals has been casted into working equations and applied to sequences of finite cylindrical fullerenes modeling the (5,5) and (10,10) single-walled capped carbon nanotubes. The behavior of DOS, LDOS, and global and local softness as functions of length and tube type is investigated in the simplest Hückel approximation. DOS-based calculation of global softness gives results that depend less on the details of the electronic structure than those based on the finite-difference approximation. Armchair single-walled nanotubes with larger diameters are softer than those with smaller diameters at the same tube length. Local softness, after fluctuations in the end-cap region, settles down within the first 20 layers of hexagons of the tube body to a constant (diameter-dependent) value.

Introduction

Within the framework of density functional theory (DFT),[1] the subfield of conceptual DFT[2−4] concentrates on the development and use of reactivity descriptors. Descriptors such as hardness, softness (global and local), and electronic and nuclear Fukui functions have been shown to be useful tools in rationalizing the global and local aspects of reactivity among others by our research group (see, for example, refs 5−12). Normally with finite systems, those quantities are obtained within the finite-difference approximation (FDA).[13] However, when the HOMO−LUMO gap vanishes, as in the case of a metal, the FDA method fails to give physically acceptable values of those descriptors. In 1985 Yang and Parr[14] identified the softness and the local softness for infinite systems such as metals with the density of states (DOS) and local density of states (LDOS) at the Fermi level, respectively. Until now, this proposition has been used in only a few cases, e.g., to study the adsorption of atoms and molecules on Si(111)-(7×7)[15] and the basicity of alkaline-exchanged zeolites[16] even though in those cases the metallic character of the substrate is absent. In contrast, the concepts of DOS and LDOS have already been applied in several studies on the electronic structure of carbon nanotubes,[17−28] without however establishing the link with global and local softness and its chemical implications.

In 1985, buckminsterfullerene, C_{60}, a new form of carbon beyond diamond and graphite, was discovered.[29] Among other new modifications of carbon, multiwalled nanotubes (MWNTs)[30] were later reported in 1991 and single-walled nanotubes (SWNTs)[31] in 1993. Since then, a large amount of work has been done to study the structural, electrical, mechanical, and chemical properties of carbon nanotubes to explore the applications of these promising materials.[32]

An SWNT can be considered as a single graphene sheet rolled up to form a hollow cylinder. The helicity and diameter of an SWNT are characterized by the roll-up vector $\mathbf{C}_h = n\mathbf{a}_1 + m\mathbf{a}_2 \equiv (n,m)$, where $\mathbf{a}_1$ and $\mathbf{a}_2$ are the graphene lattice vectors and n and m are integers.[32] There are three kinds of SWNTs, namely, the $(n,0)$ zigzag, the (n,n) armchair, and the (n,m) $(n \neq m)$ chiral carbon nanotubes. In simple Hückel theory, the (n,m) tubes are expected to be metallic if $(2n + m)/3$ is an integer and semiconducting otherwise, with a gap $\propto 1/R$, where R is the tube radius.[33−38] In more detailed tight-binding calculations, the tubes with $(2n + m)/3$ as an integer become small-band-gap semiconductors, with gaps on the order of ∼0.01 eV, except for those with $n = m$, which remain metallic.[33,36,39]

For applications, it is important to understand the effect of diameter, helicity, length, and capping of SWNTs on their electronic structure and, hence, on their chemical properties such as reactivity.

Considering the metallic nature of the (n,n) armchair carbon nanotubes, we will probe in this work the DOS, LDOS, and global and local softness approaches for the series of (5,5) and (10,10) nanotubes, as modeled by cylindrical fullerenes, i.e., capped nanotubes. The paper has two aims, on one hand, pointing out a practical procedure for calculating the DFT-based reactivity descriptors for metallic systems and, on the other hand, by varying the length and diameter of the SWNT, investigating the behavior of these quantities in the capped nanotubes considered.

In view of the presence of an extended π-system in carbon nanotubes involving a large number of carbon atoms, the classical Hückel molecular orbital (HMO) method,[40] used to rationalize and predict properties and reactivities of conjugated compounds in organic chemistry,[41] remains useful for estimating patterns of molecular orbital (MO) energies and coefficients in these all-carbon systems. It gives a simple test of the working

* To whom correspondence should be addressed. Email: pgeerlin@vub.ac.be.
† HoChiMinh City University of Technology.
‡ Vrije Universiteit Brussel.
§ University of Exeter.

10.1021/jp0343887 CCC: $25.00
Published on Web 08/09/2003

formulas for these descriptors and the factors influencing the reactivity of nanotubes.

Theoretical Aspects

The global softness S and the local softness are defined as

$$S = \frac{1}{2\eta} = \left(\frac{\partial N}{\partial \mu}\right)_{v(\vec{r})} \tag{1}$$

$$s(\vec{r}) = Sf(\vec{r}) = \left(\frac{\partial \rho(\vec{r})}{\partial \mu}\right)_{T,v(\vec{r})} \tag{2}$$

It was shown by Yang and Parr[14] that

$$S = g(\epsilon_F) \tag{3}$$

$$s(\vec{r}) = g(\epsilon_F, \vec{r}) \tag{4}$$

where S is the global softness, $s(\vec{r})$ the local softness, μ the chemical potential, ϵ_F the Fermi energy, $g(\epsilon_F)$ the DOS, and $g(\epsilon_F,\vec{r})$ the LDOS at the Fermi level.

The density of states $g(\epsilon)$ and local density of states $g(\epsilon,\vec{r})$ at energy ϵ are given by[14]

$$g(\epsilon) = \sum_i \delta(\epsilon_i - \epsilon) \tag{5}$$

$$g(\epsilon, \vec{r}) = \sum_i |\psi_i(\vec{r})|^2 \delta(\epsilon_i - \epsilon) \tag{6}$$

where ϵ_i is the energy of the molecular orbital ψ_i. To avoid the discontinuity of the δ function when applying these expressions to finite, large systems such as SWNTs, we replace the δ function by a normalized Gaussian, as in

$$\mathrm{DOS} = g(\epsilon) = \frac{1}{\Delta\sqrt{\pi}} \sum_i \exp\left[-\left(\frac{\epsilon - \epsilon_i}{\Delta}\right)^2\right] \tag{7}$$

$$\mathrm{LDOS}(k) = g(\epsilon,k) = \frac{1}{\Delta\sqrt{\pi}} \sum_i |C_{ki}|^2 \exp\left[-\left(\frac{\epsilon - \epsilon_i}{\Delta}\right)^2\right] \tag{8}$$

where Δ is the width of the Gaussian function, LDOS(k) is the local density of states at atom k, and C_{ki} and ϵ_i are the coefficients and energy of molecular orbital i. The sum is taken to run over all MOs.

At $T = 0$ K, the normalization conditions are

$$N = \int_0^\mu g(\epsilon)\, d\epsilon \tag{9}$$

$$\rho(\vec{r}) = \int_0^\mu g(\epsilon, \vec{r})\, d\epsilon \tag{10}$$

where the chemical potential μ is equal to the Fermi energy ϵ_F. According to (1) and (2) we must take the derivatives of the number of electrons N and the density with respect to the chemical potential. By using (1)−(4), (9), and (10), the global softness and the local softness can be written as[15]

$$S = \left(\frac{\partial N}{\partial \mu}\right)_{v(\vec{r})} = \lim_{\delta\mu \to 0} \frac{1}{\delta\mu} \int_\mu^{\mu+\delta\mu} g(\epsilon)\, d\epsilon \tag{11}$$

$$s(\vec{r}) = \left(\frac{\partial \rho(\vec{r})}{\partial \mu}\right)_{T,v(\vec{r})} = \lim_{\delta\mu \to 0} \frac{1}{\delta\mu} \int_\mu^{\mu+\delta\mu} g(\epsilon, \vec{r})\, d\epsilon \tag{12}$$

Generally, $\delta\mu$ could be positive or negative depending on whether the system gains or loses electrons. As metals have no band gap, the first derivative of the number of electrons with respect to the chemical potential is continuous in the vicinity of the Fermi level, leading to equality of left and right derivatives, losing the usual distinction[1,42] between s^+ and s^-. The global softness S and the condensed local softness s_k at atom k can be approximated by

$$S = \frac{1}{2b}\int_{\epsilon_F - b}^{\epsilon_F + b} g(\epsilon)\, d\epsilon = \frac{1}{2b\Delta\sqrt{\pi}} \sum_i \int_{\epsilon_F - b}^{\epsilon_F + b} \exp\left[-\left(\frac{\epsilon - \epsilon_i}{\Delta}\right)^2\right] d\epsilon$$

$$= \frac{1}{4b} \sum_i \left[\mathrm{erf}\left(\frac{\epsilon_F + b - \epsilon_i}{\Delta}\right) - \mathrm{erf}\left(\frac{\epsilon_F - b - \epsilon_i}{\Delta}\right)\right] \tag{13}$$

$$s_k = \frac{1}{2b\Delta\sqrt{\pi}} \sum_i |C_{ki}|^2 \int_{\epsilon_F - b}^{\epsilon_F + b} \exp\left[-\left(\frac{\epsilon - \epsilon_i}{\Delta}\right)^2\right] d\epsilon$$

$$= \frac{1}{4b} \sum_i |C_{ki}|^2 \left[\mathrm{erf}\left(\frac{\epsilon_F + b - \epsilon_i}{\Delta}\right) - \mathrm{erf}\left(\frac{\epsilon_F - b - \epsilon_i}{\Delta}\right)\right] \tag{14}$$

where the error function erf(z) has been used for evaluation of definite integrals:

$$\int_{z_1}^{z_2} e^{-s2}\, ds = \frac{\sqrt{\pi}}{2}[\mathrm{erf}(z_2) - \mathrm{erf}(z_1)] \tag{15}$$

The values obtained from (13) and (14) can then be compared to those obtained from the FDA, in which three forms of the local softness can be distinguished:

$$S_{\mathrm{FDA}} = (\epsilon_{\mathrm{LUMO}} - \epsilon_{\mathrm{HOMO}})^{-1}$$

$$s_k^{+}(\mathrm{FDA}) = |C_{k,\mathrm{LUMO}}|^2 S_{\mathrm{FDA}}$$

$$s_k^{-}(\mathrm{FDA}) = |C_{k,\mathrm{HOMO}}|^2 S_{\mathrm{FDA}}$$

$$s_k^{0}(\mathrm{FDA}) = \frac{1}{2}(s_k^{+} + s_k^{-}) \tag{16}$$

Computational Details

An icosahedral fullerene can be used as a template for an infinite series of carbon nanotubes formed by cutting the parent molecule along an equator and inserting a tubular portion of hexagons.[32] The (5,5) series has formula C_{60+10n} with symmetries alternating between D_{5h} (n = 1, 3, 5, ...) and D_{5d} (n = 2, 4, 6, ...). This series can be generated from C_{60} by adding five hexagons (a 10-atom belt) when n increases by 1. Similarly, the (10,10) series having formula $C_{200+20n}$ is capped with the hemisphere of the D_{5h} C_{200} fullerene, and a belt of 20 carbon atoms is added with each increment of 1 in n (see Figure 1a). For simplicity, we chose the D_{5h} (n = 2, 4, 6, ...) cases to probe the effect of the SWNT diameter.

The coefficients and energies of the molecular orbitals are taken from HMO calculations[40] using adjacency lists generated by the spiral algorithm,[43] for unwinding the surface of a capped nanotube in a continuous spiral strip of edge-sharing five- and six-membered rings. The energy of the ith MO is, as usual, written in the form

$$\epsilon_i = \alpha + x_i\, (\beta < 0) \tag{17}$$

where α is the Coulomb integral and β the resonance integral.[40] With $x_i = x_F = x_{\mathrm{HOMO}}$, (17) gives the Fermi energy.

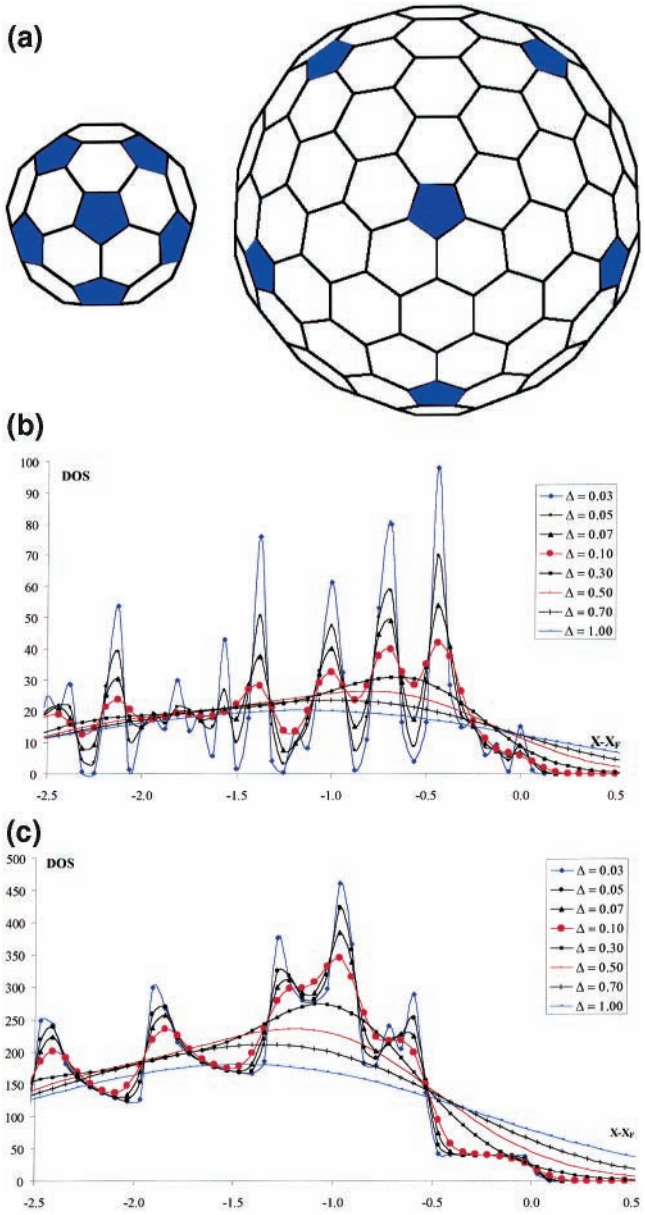

Figure 1. (a, top) View along the C_5 axis of C_{70} and D_{5h} C_{240}. (b, middle) Effect of Δ (eV) on the DOS for C_{120} (only occupied states are considered). (c, bottom) Effect of Δ (eV) on the DOS for C_{1060} (only occupied states are considered).

For uniformity, the width of the Gaussian function Δ and the range b of the integrals in (13) and (14) are written as

$$\Delta = y\beta \tag{18}$$

$$b = z\beta \tag{19}$$

In this work, we adopt the value of $|\beta| \approx 0.8$ eV/molecule obtained from the delocalization energy of benzene[41] to convert the values of Δ and b to electronvolts.

Results and Discussion

1. Effect of the Width Δ and the Range *b* on the DOS. The value of the width Δ affects the shape and amplitude of the Gaussian function, with the δ function recovered in the limit $\Delta \rightarrow 0$. Santos et al.[16] used the value of 0.5 eV for Δ in the study of alkaline-exchanged zeolites, whereas Rochefort et al.[17] chose energy resolution $\omega = 0.2$ eV (corresponding to $\Delta = 0.14$ eV) in their study of carbon nanotubes. We have studied the effect of Δ in the range of 0.03−1.00 eV on the DOS for the series consisting of C_{60}, C_{120}, C_{360}, C_{560}, and C_{1060}. The results are reported in Figure 1b for C_{120} and Figure 1c for C_{1060}. It turns out that when Δ is equal to 0.1 eV, the shape of the Gaussian function lies on the borderline between narrow and shallow curves. The same conclusion is observed for other structures. Therefore, we selected the value of 0.1 eV for Δ.

The value of the range b in the integrals in (13) and (14) also poses problems for the calculation of the global and local softness. According to (11) and (12), the value of b should be chosen to be as small as possible. However, taking into account the interval between consecutive MO energies of the nanotubes and the differences between the occupied and unoccupied states close to the Fermi level, we selected a value of 0.1 eV for b. The MO energy levels in HMO calculations for carbon nanotubes lie in the range from $+3\beta$ to -3β. In this work, we consider the global and local softness of SWNTs having more than 500 carbon atoms, for a typical interval between consecutive MO energies is $6\beta/500 \approx 0.01$ eV, and thus, even for the smallest system the selected range b always includes a number of MO levels. In studying the adsorption of atoms and molecules on Si(111)-(7×7), Joannopoulos et al.[15] used a value of ±0.5 eV for b.

2. Electronic Structures. In an armchair SWNT, the carbon atoms are distributed in parallel planes perpendicular to the tube axis, starting and ending with layers containing pentagons. It has been reported[17,44−46] that the HOMO−LUMO gap (band gap) oscillates as a function of the nanotube length depending on the number of single circular planes (sections) of carbon atoms packed along the length of the SWNT. Three kinds of band-gap variation are found corresponding to an SWNT with $3N$, $3N - 2$, and $3N - 1$ sections.[17] The oscillations of the band gap can be explained in terms of the changes in the bonding characteristics of the HOMO and LUMO orbitals along and around the tube axis of the SWNT.[17]

The (5,5) armchair SWNT generated from the formula C_{60+10n} can be classified in three forms depending on its electronic structure: A ($n = 3, 6, 9, ..., 3N$), B ($n = 1, 4, 7, ..., 3N - 2$), and C ($n = 2, 5, 8, ..., 3N - 1$). We define N_{sect} ($= n$ in C_{60+10n} or $C_{200+20n}$) as the number of sections added to the parent molecules. The distance between successive sections in the nanotube is 1.22 Å.[17]

Figure 2a presents the band-gap variation as a function of N_{sect} for both (5,5) and (10,10) series. It can be seen that the D_{5h} (10,10) SWNT of formula $C_{200+20n}$ can also be divided into three subtypes corresponding to different band-gap patterns: A′ ($n = 3, 6, 9, ..., 3N$), B′ ($n = 1, 4, 7, ..., 3N - 2$), and C′ ($n = 2, 5, 8, ..., 3N - 1$). As Figure 2a also shows, the band-gap values in all six subseries converge to zero upon elongation of the nanotubes. One way of removing this simple size dependence of the gap is to calculate the T value, defined by Aihara et al.[47,48] as the HOMO−LUMO gap multiplied by the number of conjugated atoms, and proposed as an index of kinetic stability for fullerene systems. As can be seen from Figure 2b, T makes a clear separation between subseries. On this criterion, types A and C′ are predicted to have higher kinetic stability than the others.

Although simple Hückel theory predicts metallic behavior only for the infinite (n,n) armchair SWNTs, Rochefort et al.[17] estimated that the (6,6) nanotubes without end caps would already be metallic (band gap ≈ 0) if longer than 450 Å, $N_{sect} \approx 370$ (MNDO), or 100 Å, $N_{sect} \approx 82$ (DFT and EHMO). Figure 2a shows that the band gap falls below 0.1β (∼0.08 eV) when N_{sect} exceeds 30 in both (5,5) and (10,10) series, and it seems

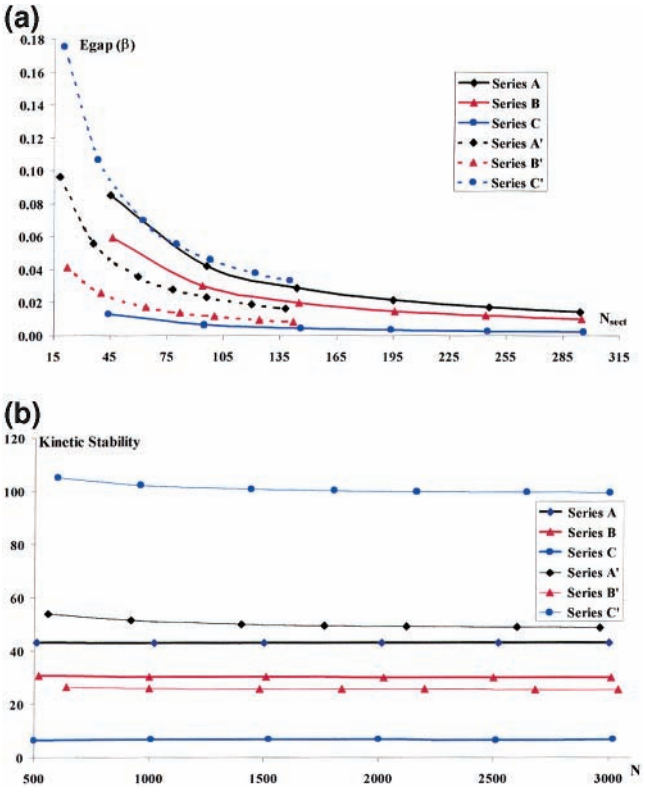

Figure 2. (a, top) Band-gap variation with respect to the number of added sections for (5,5) (full lines) and (10,10) (dashed lines) armchair SWNTs. (b, bottom) Kinetic stability with respect to the number of atoms N for (5,5) (full lines) and (10,10) (dashed lines) armchair SWNTs.

that the tubes are starting to exhibit the typical characteristics of the infinite system. Also by the time this size is reached, a significant difference can be seen between FDA-based and DOS-based calculations of softness. In what follows, we consider only SWNTs having N_{sect} larger than 30.

3. Global Softness (S). The global softness calculated from eq 16 (S_{FDA}) and from eq 13 (S_{DOS}) as a function of N_{sect} are displayed in Figure 3a, with $N_{sect} > 45$ (>500 carbon atoms) for the (5,5) series. The figure with $N_{sect} > 62$ (>1400 carbon atoms) for the (10,10) series is given in the Supporting Information. The FDA-based values of global softness show an inverse proportion to the band gap, i.e., $S_A < S_B < S_C$ for (5,5) and $S_{C'} < S_{A'} < S_{B'}$ for (10,10).

It is notable that the DOS-based global softness, for all three kinds of electronic structure, falls on the same line, as opposed to the three different lines produced by the FDA method. The strongly oscillatory behavior of S_{FDA} with increasing number of atoms reflects its reciprocal relation with the band gap (E_g). The S_{FDA} values are thus very sensitive to variation in E_g, especially at a small gap. When the gap vanishes, S_{FDA} goes to infinity. In contrast, S_{DOS} depends only on the DOS in the neighborhood of the Fermi level; in turn, the latter depends on the MO degeneracy and energy intervals close to this level. Consequently, the overall picture of S_{DOS} is that of a monotonically increasing curve with the number of atoms. As can be seen from Figure 3b, the global softness S_{DOS} also increases with increasing diameter of the nanotubes at a given length. The small slope of the variation of the global softness with N_{sect} is similar and decreases in the two series, suggesting a plateau of softness as N_{sect} tends to infinity. S_{DOS}, rather than S_{FDA}, seems to be the correct quantity to represent the global softness of infinite systems such as metals and carbon nanotubes.

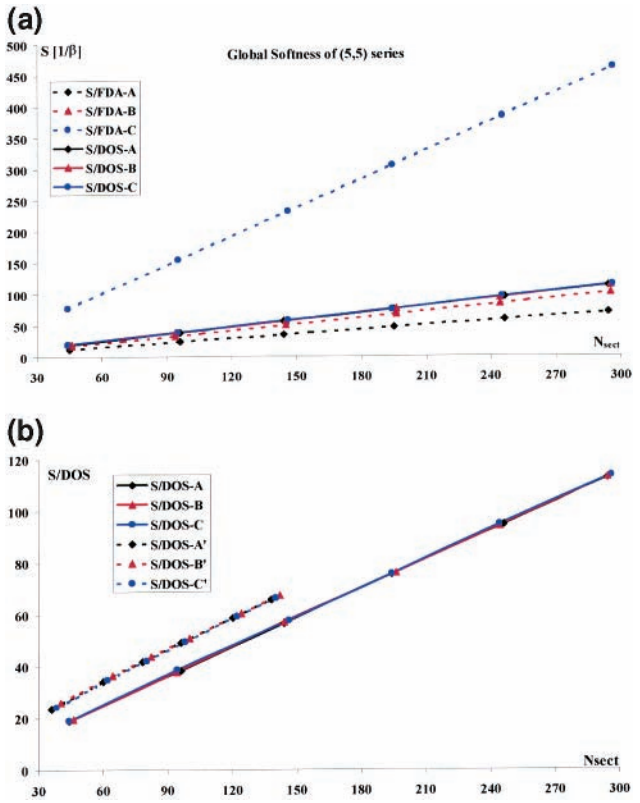

Figure 3. (a, top) Global softness as a function of N_{sect} for (5,5) armchair SWNTs. (b, bottom) S_{DOS} in units of $[1/\beta]$ as a function of N_{sect} for (5,5) (full lines) and (10,10) (dashed lines) armchair SWNTs.

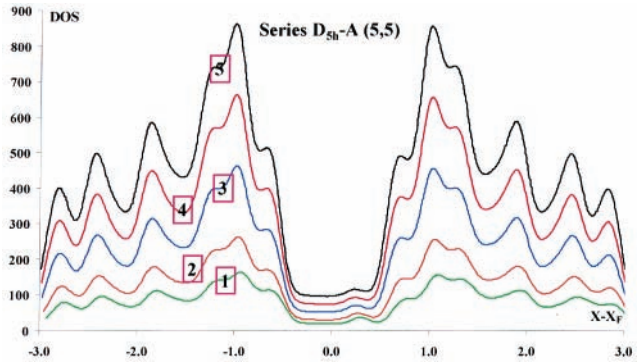

Figure 4. DOS versus N_{sect} and energies for the D_{5h} A (5,5) SWNT series. The numbers correspond to (1) $N_{sect} = 45$ or C_{510}, (2) $N_{sect} = 75$ or C_{810}, (3) $N_{sect} = 135$ or C_{1410}, (4) $N_{sect} = 195$ or C_{2010}, and (5) $N_{sect} = 255$ or C_{2610}.

4. DOS. Figure 4 plots the behavior of DOS as a function of the energy and N_{sect} for the subsets of the (5,5) and (10,10) series with the highest T values (i.e., A and C′, respectively) (the case of the (10,10) series is shown in the Supporting Information). Features of the DOS, such as the position and intensity of the main DOS peaks and the flatness in magnitude around the Fermi level, are similar within the two series. Moreover, between short and long nanotubes, the DOS simply shows an augmentation in magnitude at some specific energies.

Against these similarities, some significant differences between the two series are apparent. The DOS curve in the (5,5) series shows the existence of clearly differentiated main peaks, whereas in the (10,10) series there is only one main peak at $|X - X_F| = 1\beta$. At each value of N_{sect} the DOS in the (10,10) series is higher than in the (5,5) series, as an effect of the shorter intervals between successive MO energies.

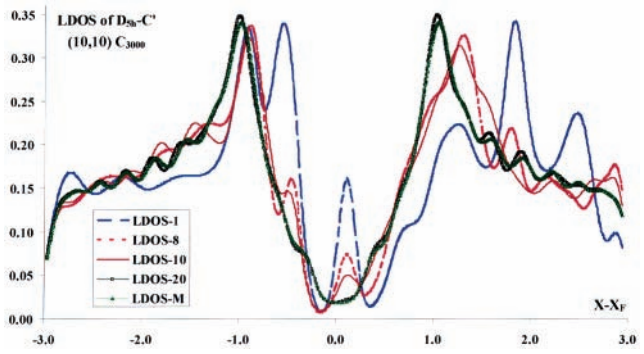

Figure 5. LDOS at different layers for the D_{5h} C′ (10,10) SWNT with $N_{sect} = 140$ or C_{3000}.

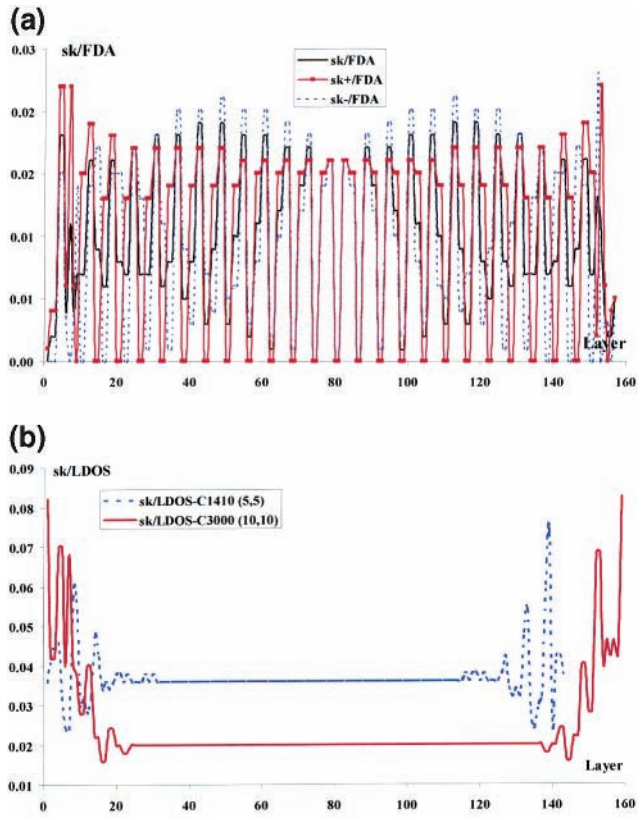

Figure 6. (a, top) s_k(FDA) at different layers for the D_{5h} C′ (10,10) SWNT with $N_{sect} = 140$ or C_{3000}. (b, bottom) s_k(LDOS) at different layers for the D_{5h} A C_{1410} (5,5) and D_{5h} C′ C_{3000} (10,10) SWNTs.

5. LDOS and Local Softness (s_k). As mentioned in section 2, the carbon atoms in an armchair SWNT are distributed in parallel planes (layers) perpendicular to the tube axis. By Euler's theorem, each end cap contains six pentagons, perturbing the hexagonal graphene network. In the (5,5) series capped with halves of C_{60}, the pentagons are associated with layers 1, 2, 3, 4, $L - 3$, $L - 2$, $L - 1$, and L, where L is the number of SWNT total layers. In the (10,10) series, the pentagons are associated with layers 1, 7, 8, 9, $L - 8$, $L - 7$, $L - 6$, and L (see Figure 1a).

The LDOS and local softness (s_k(FDA) and s_k(LDOS)) were calculated for the symmetry-unique carbon in each layer of each SWNT considered. Representative LDOSs are displayed in Figure 5 for $N_{sect} = 140$ (C_{3000}) in the (10,10) series (the $N_{sect} = 135$ (C_{1410}) case in the (5,5) series is given in the Supporting Information). The symbol LDOS-*i* represents the LDOS value in layer *i*, and LDOS-M is the value for the middle layer of the tube.

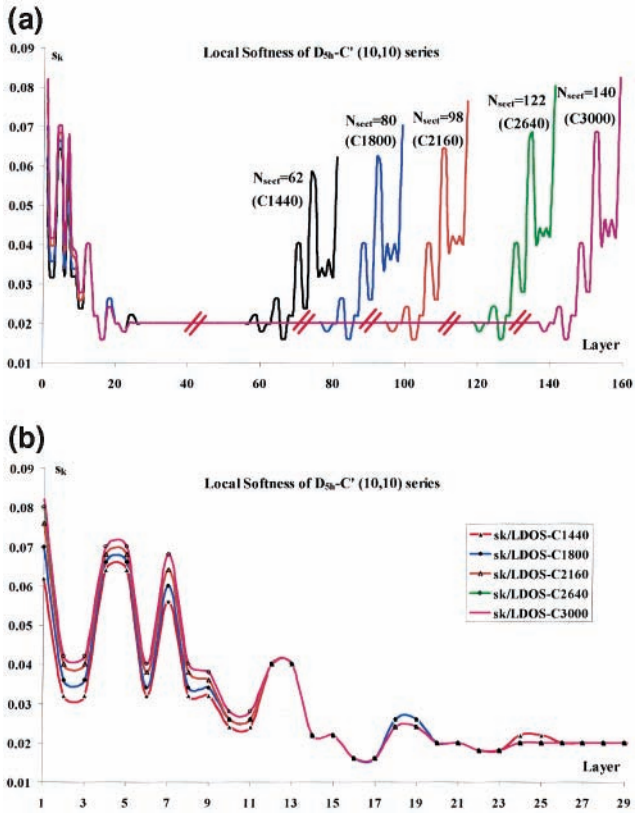

Figure 7. (a, top) s_k(LDOS) as a function of layers for the D_{5h} C′ (10,10) SWNT series. In each case the abscissa shows only the portion of the curve corresponding to the termination of the oscillatory behavior. Portions are separated by the "//" symbol. (b, bottom) Expanded view of s_k(LDOS) in (a) at a low number of layers.

Figure 5 shows near equality of LDOS curves for layers far from the end cap, for example, layer 20. In contrast, the LDOS curves for the layers in or near the end cap show different patterns, with a strong LDOS peak at the Fermi level. LDOS values at layers 1 and 3 in the (5,5) SWNT (not shown) and 1 and 8 in the (10,10) SWNT are the largest in the vicinity of the Fermi level. The energy of the peaks shows these layers to be associated with the π-electron deficiency induced by the pentagons. The carbon atoms in these layers show higher reactivity and greater local softness than the others. As the diameter increases, this signature of π-electron deficiency is reduced.

Results for local softness calculated from FDA and LDOS methods are displayed in Figure 6a (the (5,5) analogue of Figure 6a being given in the Supporting Information).

The calculated values of s_k(FDA) show a strong oscillation of local softness from one layer to another along the tube axis. These results together with those for the softness itself strongly suggest that FDA-based descriptors fail when applied to very large systems. In contrast, s_k(LDOS) displays a short-lived perturbation at layers near the end cap and reaches a constant value for layers in the middle of the tube. As a consequence, it is of interest to know from which layer the local softness (s_k(LDOS)) will reach a constant value without being affected by the end cap. Calculations of s_k(LDOS) for the two series (Figure 7a,b) explored this point.

Figure 7a indicates that all the values of s_k(LDOS) at the middle layers reach a constant with increasing number of atoms or N_{sect} [e.g., $s_k = 0.036$ in the (5,5) series] which is equal to 0.020 in the (10,10) series. For the (5,5) series, shown in the Supporting Information, the corresponding value is $s_k = 0.036$.

The lower constant of local softness in the (10,10) SWNT is expected in Hückel theory from the nature of the HOMO and LUMO.

From the expanded view in Figure 7b, it can be seen that constant s_k(LDOS) is already reached by layer 20 in the (10,10) series (the same value as in the (5,5) series, Supporting Information), irrespective of the difference in diameter. It is therefore plausible to predict the pattern of local softness of an infinite armchair SWNT; after end effects have died away, from layer 20 down to layer $L - 19$ the local softnesses will be all equal, with their constant value depending on the diameter of the tube. In the perfect infinite tube, where all sites are equivalent by symmetry, everywhere the local softness will be equal to the total softness divided by the volume of the system.

Conclusions

In summary, the present work compared the global and local softness on the basis of the FDA approach and the concept of DOS and LDOS, all within the context of HMO calculations, for fullerenes as analogues of large armchair carbon nanotubes. FDA-based values show different patterns of softness corresponding to the different electronic and geometric structures, and an oscillatory behavior of the local softness along the tube axis. DOS-based global softness increases monotonically with the number of atoms. Armchair SWNTs of larger diameters are softer than smaller tubes of the same length. The LDOS-based local softness values oscillate in the cap portion of the tube, but reach a constant within the first 20 or so layers. This constant value depends on the diameter of the nanotube. It is suggested that the DOS- and LDOS-based descriptors may be promising reactivity indices for studying the chemistry of large finite systems such as carbon nanotubes.

Acknowledgment. We thank the Fund for Scientific Research FWO-Vlaanderen for financial support, and the Vrije Universiteit Brussel (VUB) computer center for help with calculations. L.T.N. thanks the VUB for a one-year doctoral fellowship. P.G. and G.V.L. thank Professor J. C. Charlier (Université Catholique de Louvain, Belgium) for stimulating discussions.

Supporting Information Available: Figures showing the global softness as a function of N_{sect} for (10,10) SWNTs, DOS versus N_{sect} and energies for D_{5h} C′ (10,10) SWNTs, and LDOS at different layers, s_k(FDA) at different layers, and s_k(LDOS) as a function of layers (along with its expanded view) for D_{5h} A (5,5) SWNTs. This material is available free of charge via the Internet at http://pubs.acs.org.

References and Notes

(1) Parr, R. G.; Yang, W. *Density Functional Theory of Atoms and Molecules*, Oxford University Press: New York, 1989.
(2) Parr, R. G.; Yang, W. T. *Annu. Rev. Phys. Chem.* **1995**, *46*, 701.
(3) Chermette, H. *J. Comput. Chem.* **1999**, *20*, 129.
(4) (a) Geerlings, P.; De Proft, F.; Langenaeker, W. *Adv. Quantum Chem.* **1999**, *33*, 303. (b) Geerlings, P.; De Proft, F.; Langenaeker, W. *Chem. Rev.* **2003**, *103*, 1793.
(5) Nguyen, L. T.; Le, T. N.; De Proft, F.; Chandra, A. K.; Langenaeker, W.; Nguyen, M. T.; Geerlings, P. *J. Am. Chem. Soc.* **1999**, *121*, 5992.
(6) Nguyen, L. T.; De Proft, F.; Nguyen, M. T.; Geerlings, P. *J. Org. Chem.* **2001**, *66*, 4316.
(7) Nguyen, L. T.; De Proft, F.; Chandra, A. K.; Uchimaru, T.; Nguyen, M. T.; Geerlings, P. *J. Org. Chem.* **2001**, *66*, 6096.
(8) Balawender, R.; Geerlings, P. *J. Chem. Phys.* **2001**, *114*, 682.
(9) Balawender, R.; De Proft, F.; Geerlings, P. *J. Chem. Phys.* **2001**, *114*, 4441.
(10) Damoun, S.; Van de Woude, G.; Mendez, F.; Geerlings, P. *J. Phys. Chem. A* **1997**, *101*, 886.
(11) Geerlings, P.; De Proft, F. *Int. J. Quantum Chem.* **2000**, *80*, 227.
(12) De Proft, F.; Geerlings, P. *Chem. Rev.* **2001**, *101*, 1451.
(13) Yang, W.; Mortier, W. J. *J. Am. Chem. Soc.* **1986**, *108*, 5708.
(14) Yang, W.; Parr, R. G. *Proc. Natl. Acad. Sci. U.S.A.* **1985**, *82*, 6723.
(15) Brommer, K. D.; Galván, M.; Dal Pino, A.; Joannopoulos, J. D. *Surf. Sci.* **1994**, *314*, 57.
(16) Santos, J. C.; Contreras, R.; Chamorro, E.; Fuentealba, P. *J. Chem. Phys.* **2002**, *116*, 4311.
(17) Rochefort, A.; Salahub, D. R.; Avouris, P. *J. Phys. Chem. B* **1999**, *103*, 641.
(18) Itkis, M. E.; Niyogi, S.; Meng, M. E.; Hamon, M. A.; Hu, H.; Haddon, R. C. *Nano Lett.* **2002**, *2*, 155.
(19) Östling, D.; Tománek, D.; Rosén, A. *Phys. Rev. B* **1997**, *55*, 13980.
(20) Rochefort A.; Avouris, P. *Nano Lett.* **2002**, *2*, 253.
(21) Han, S.; Ihm, J. *Phys. Rev. B* **2000**, *61*, 9986.
(22) Rochefort, A.; Salahub, D. R.; Avouris, P. *Chem. Phys. Lett.* **1998**, *297*, 45.
(23) Srivastava, D.; Brenner, D. W.; Schall, J. D.; Ausman, K. D.; Yu, M. F.; Ruoff, R. S. *J. Phys. Chem. B* **1999**, *103*, 4330.
(24) Odom, T. W.; Huang, J.-L.; Kim, P.; Lieber, C. M. *J. Phys. Chem. B* **2000**, *104*, 2794.
(25) Carroll, D. L.; Redlich, P.; Ajayan, P. M.; Charlier, J. C.; Blase, X.; DeVita, A.; Car, R. *Phys. Rev. Lett.* **1997**, *78*, 2811.
(26) Mintmire, J. W.; White, C. T. In *Density Functional Theory and its Application to Materials*; Van Doren, V., Van Alsenoy, C., Geerlings, P., Eds.; American Institute of Physics Conference Proceedings; AIP: New York, 2001; pp 98−116.
(27) Zhou, G.; Duan, W. H.; Gu, B. L.; Kawazoe, Y. *J. Chem. Phys.* **2002**, *116*, 2284.
(28) Kim, C.; Kim, B.; Lee, S. M.; Jo, C.; Lee, Y. H. *Phys. Rev. B* **2002**, *65*, 165418.
(29) Kroto, H. W.; Heath, J. R.; Brien, S. C. O.; Curl, R. F.; Smalley, R. E. *Nature* **1985**, *318*, 162.
(30) Iijima, S. *Nature* **1991**, *354*, 56.
(31) Iijima S.; Ichihashi, T. *Nature* **1993**, *363*, 603.
(32) Dresselhaus, M. S.; Dresselhaus, G.; Eklund, P. C. *Science of Fullerenes and Carbon Nanotubes*; Academic Press: San Diego, 1996.
(33) Hamada, N.; Sawada, S.; Oshiyama, A. *Phys. Rev. Lett.* **1992**, *68*, 1579.
(34) Mintmire, J. W.; Dunlap, B. I.; White, C. T. *Phys. Rev. Lett.* **1992**, *68*, 631.
(35) Saito, R.; Fujita, M.; Dresselhaus, G.; Dresselhaus, M. S. *Appl. Phys. Lett.* **1992**, *60*, 2204.
(36) Blase, X.; Benedict, L. X.; Shirley, E. L.; Louie, S. G. *Phys. Rev. Lett.* **1994**, *72*, 1878.
(37) Kane C. L.; Mele, E. J. *Phys. Rev. Lett.* **1997**, *78*, 1932.
(38) Crespi, V. H.; Cohen, M. L.; Rubio, A. *Phys. Rev. Lett.* **1997**, *79*, 2093.
(39) Palser, A. H. R. Theoretical Properties of Nanotubes. D.Phil. Thesis, University of Oxford, 2000. Small gaps for the larger tubes of this type with $n \neq m$ are also predicted by LDA calculations in ref 36.
(40) Streitwieser, A. *Molecular Orbital Theory for Organic Chemists*; Wiley: New York, 1961.
(41) Levine, I. N. *Quantum Chemistry*, 4th ed.; Prentice Hall: Englewood Cliffs, NJ, 1991.
(42) Parr R. G.; Yang, W. T. *J. Am. Chem. Soc.* **1984**, *106*, 4049.
(43) Fowler, P. W.; Manolopoulos, D. E. *An Atlas of Fullerenes*; Oxford University Press: Oxford, 1995.
(44) Yamabe, T.; Imade, M.; Tanaka, M.; Sato, T. *Synth. Met.* **2001**, *117*, 61.
(45) Liu, L.; Jayanthi, C. S.; Wu, S. Y. *Chem. Phys. Lett.* **2002**, *357*, 91.
(46) Van Lier, G.; Fowler, P. W.; De Proft, F.; Geerlings, P. *J. Phys. Chem. A* **2002**, *106*, 5128.
(47) Yoshida, M.; Aihara, J. *Phys. Chem. Chem. Phys.* **1999**, *1*, 227.
(48) Aihara, J. *Phys. Chem. Chem. Phys.* **2000**, *2*, 3121.